Proceedings of Montreal 2018
Global Power and Propulsion Forum
7th – 9th May, 2018
www.pps.global

GPPS-NA-2018-163

AN IMPROVED IMAGE PROCESSING APPROACH FOR MACHINERY FAULT DIAGNOSIS

Kar Hoou Hui
Universiti Teknologi Malaysia
huikarhoou@gmail.com
Kuala Lumpur, Malaysia

Ching Sheng Ooi
Universiti Teknologi Malaysia
chingshengooi@gmail.com
Kuala Lumpur, Malaysia

Wai Keng Ngui
Universiti Malaysia Pahang
waikeng@ump.edu.my
Pekan, Pahang, Malaysia

Meng Hee Lim
Universiti Teknologi Malaysia
mhlim.kl@utm.my
Kuala Lumpur, Malaysia

Mohd Salman Leong
Universiti Teknologi Malaysia
salman.kl@utm.my
Kuala Lumpur, Malaysia

ABSTRACT

Wavelet analysis has been proven to be effective in analysing non-stationary vibration signals. However, the interpretation of the wavelet analysis results, such as a wavelet scalogram, requires high levels of knowledge and experience, which remains a great challenge to practitioners in the field. Recently, the rapid development and advancement of image processing technologies have shed new light on this challenge. In this study, image features such as Harris Stephens (Harris); speeded-up robust features (SURFs); and binary, robust, invariant, scalable keypoints (BRISKs) were obtained from a red, green, and blue (RGB) colour-filtered wavelet scalogram. Each colour filter generates a set of image features from an RGB-filtered wavelet scalogram. Then, the features were utilised as inputs to the fault classifier, namely the support vector machine (SVM), for fault classification. However, there will be a situation where the classification results from the fault classifier, based on the image generated from the different colour filters, are contradictory to each other. No conclusion can thus be made in these situations. This paper employed the Dempster-Shafer (DS) theory to refine the contradicting results and provide an ultimate conclusion to the machine condition. Therefore, the proposed method has improved the fault classification accuracy from 69% to 78%.

INTRODUCTION

The vibration signals that are collected from turbine blades, bearings, and gears are usually non-stationary signals. Wavelet analysis has emerged as a powerful tool for non-stationary signal analysis (Konar and Chattopadhyay, 2011; Bayram and Şeker, 2013; Li *et al.*, 2013; Du *et al.*, 2014; Jamadar and Vakharia, 2016). However, the interpretation of a wavelet map is not as simple as that of a frequency spectrum (Ngui *et al.*, 2017). It is highly dependent on the knowledge and experience of the personnel. **Figure 1** illustrates an example of a wavelet scalogram for different types of bearing faults. The difficulty in interpreting a wavelet scalogram has constrained its development and application in the field. Recent developments and advancements of image processing and machine learning technologies have shed new light on this challenge. The adaptation of these technologies in machinery fault classification seems promising. This study proposes decomposing a wavelet scalogram by red, green, and blue (RGB) colour filters. Then, a set of image features, including features from an accelerated segment test (FAST); minimum eigenvalues (MinEigen); Harris Stephens (Harris); speeded-up robust features (SURFs); binary, robust, invariant, scalable keypoints (BRISKs); and maximally stable extremal regions (MSERs), are extracted from each filtered wavelet scalogram. Each colour-filtered wavelet scalogram may be sensitive toward certain types of faults, and the fault classification result generated based on each colour filter may be contradictory. Therefore, the Dempster-Shafer (DS) theory is employed to refine the contradicting results in order to provide a final classification result.

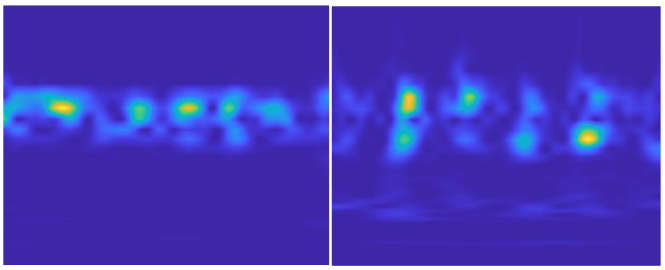

Figure 1. Wavelet Scalogram of Rolling Element Fault (left) and Inner Raceway Fault (right)

DEMPSTER-SHAFER THEORY

The concept of the DS theory was introduced by Arthur P. Dempster (1967), and it was subsequently completed by Glenn Shafer (1976). It is a mathematical theory that deals with uncertain information reasoning. It allows for the combination of evidence from multiple sources, and it provides a measure of confidence (belief function, *Bel*) that a given event will occur. Let Θ be a finite set of possible answers and ϕ represent an empty set; the belief function should satisfy the three axioms represented by Equations 1-3.

$$\mathrm{Bel}(\phi) = 0 \quad (1)$$

$$\mathrm{Bel}(\Theta) = 1 \quad (2)$$

$$\mathrm{Bel}\left(\bigcup_{i=1}^{n} A_i\right) \geq \sum_{I \subset \{1,2,\ldots,n\}} (-1)^{|I|+1} \mathrm{Bel}\left(\bigcap_{i \in I} A_i\right) \quad (3)$$

The DS theory consists of three important parameters, namely the mass function (m), belief function (*Bel*), and plausibility (*Pl*). Mass function (m) is a basic probability assignment that measures the belief that is committed exactly to a subset. Belief function (*Bel*) is a lower probability that measures the total belief mass that is confined to a subset, while plausibility (*Pl*) is a higher probability that measures the total belief mass that can move into a subset.

The most recent applications of the DS theory can be found in the fields of medical diagnostics (Guil and Marín, 2013), aviation (Phillips and Diston, 2011), machinery condition monitoring and fault diagnosis (Cao *et al.*, 2013; He *et al.*, 2014), maintenance management (Potes Ruiz, Kamsu-Foguem and Noyes, 2013), chemical engineering (Natarajan and Srinivasan, 2014), defence (Avci, 2013), the power generation industry (Bhalla, Bansal and Gupta, 2013), and engineering design (Browne *et al.*, 2013), to name a few. To date, the DS theory has been proven to be effective in combining evidence to provide a high level of confidence in the occurrence of an event.

DATA COLLECTION

The vibration signals in the study were downloaded from the Case Western Reserve University Bearing Data Centre website to represent rolling element bearing in healthy and faulty conditions, such as a rolling element fault, an inner raceway fault, and an outer raceway fault. The test rig was constructed by a 2-HP motor, a torque transducer, and a dynamometer. The test rig arrangement is presented in **Figure 2**. The motor was operated at 1,750 rpm with 1-HP loading. Vibration signals were sampled at 12 kHz by an accelerometer that was attached to the bearing housing.

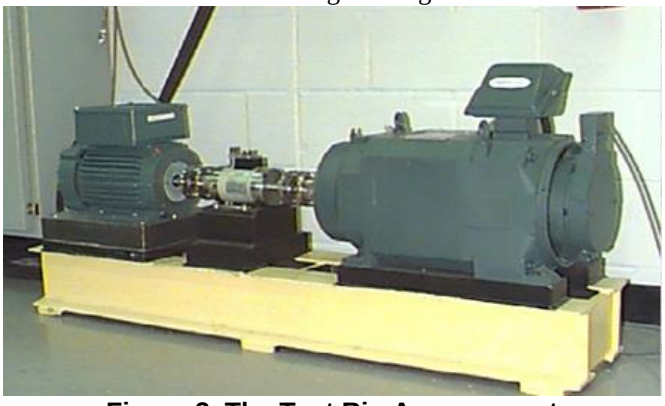

Figure 2. The Test Rig Arrangement

A total of 400 sets of wavelet scalograms were generated by continuous wavelet transform (CWT) from the raw, continuous vibration signal collected from a 7-mil fault diameter with a 1-HP loading. Then, the 400 sets of wavelet scalograms were split into two groups of data; one was used to synthesize the machine learning model (the training phase), while the other group was used to validate the synthesized machine learning model (the testing phase). The distribution of the vibration dataset in this study is tabulated in **Table 1**.

Table 1. Vibration Data Distribution

Bearing condition	Training data	Testing data
Healthy	50	50
Rolling element fault	50	50
Inner raceway fault	50	50
Outer raceway fault	50	50

IMAGE FEATURE EXTRACTION

Before proceeding to examine the performance of the classifier, it is important to explain the process of image feature extraction. In this study, an RGB filter will be applied to filter an original wavelet scalogram (**Figure 3**); then, six standardized image features in *Matlab* software were used to extract the image features of each colour-filtered wavelet scalogram. These features specifically represent the characteristics of each wavelet scalogram for different bearing conditions. **Table 2** summarises all the image features that were extracted in this study and their characteristic values.

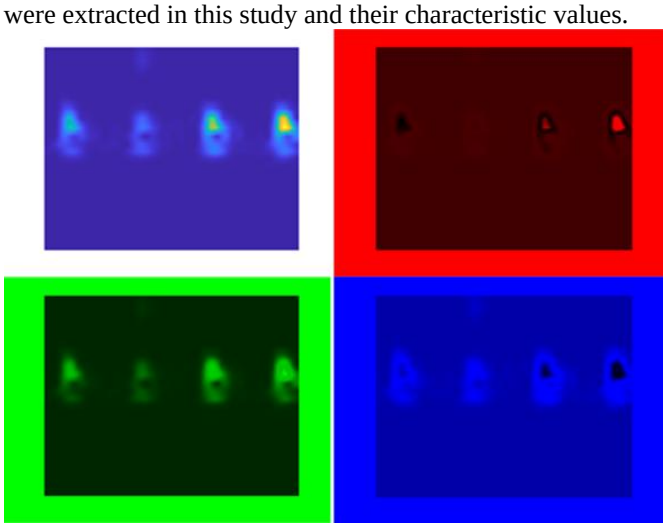

Figure 3. Example of RGB-Filtered Wavelet Scalogram

Table 2. Image Features from each Wavelet Scalogram

No.	Feature	Characteristic Value
1	Features from FAST	Corner Points
2	Minimum Eigenvalues	Corner Points
3	Harris Stephens	Corner Points

4	Speeded-Up Robust Features	Blob
5	Binary Robust Invariant Scalable Keypoints	Multiscale Corner
6	Maximally Stable Extremal Regions	Regions

RESULTS

The SVM remains one of the most favourable classifiers in machine learning due to its capability of handling a high number of input features with low sampling data sets. However, its classification accuracy reduces significantly in multi-fault classification as it was originally designed for binary classification. Therefore, the SVM-DS model (Hui *et al.*, 2017) was employed in this paper as a multi-fault classifier as a result of its outstanding performance in multi-fault classification. **Tables 2 to 4** list the confusion matrices of each colour-filtered wavelet scalogram. Their classification accuracies ranged from 61.5% to 73.5%. **Table 5** summarises the sensitivity of each colour-filtered wavelet scalogram to different bearing conditions. The analysis results demonstrate that the green colour-filtered wavelet scalogram is more sensitive to healthy or rolling element fault bearing, whilst the blue colour-filtered wavelet scalogram is more sensitive to inner or outer raceway fault bearing. Therefore, the best classification results could not be obtained by focusing on any of the colour-filtered wavelet scalograms. This paper proposes a decision-making model in the next section that fully utilises the information obtained from each colour-filtered wavelet scalogram to make an ultimate decision on the machine health condition.

Table 2. Confusion Matrix for Testing Phase (Red Colour-Filtered Wavelet Scalogram)

Condition		Actual			
		1	2	3	4
Prediction	1 (healthy)	48	1	0	0
	2 (rolling element fault)	2	21	6	9
	3 (inner raceway fault)	0	11	41	4
	4 (outer raceway fault)	0	17	3	37
Sensitivity (%)		96.0	42.0	82.0	74.0
Accuracy (%)		73.5			

Table 3. Confusion Matrix for Testing Phase (Green Colour-Filtered Wavelet Scalogram)

Condition		Actual			
		1	2	3	4
Prediction	1 (healthy)	49	3	2	1
	2 (rolling element fault)	0	28	8	18
	3 (inner raceway fault)	0	7	29	14
	4 (outer raceway fault)	1	12	11	17
Sensitivity (%)		98.0	56.0	58.0	34.0
Accuracy (%)		61.5			

Table 4. Confusion Matrix for Testing Phase (Blue Colour-Filtered Wavelet Scalogram)

Condition		Actual			
		1	2	3	4
Prediction	1 (healthy)	48	0	0	2
	2 (rolling element fault)	0	4	0	2
	3 (inner raceway fault)	0	26	48	5
	4 (outer raceway fault)	2	20	2	41
Sensitivity (%)		96.0	8.0	96.0	82.0
Accuracy (%)		70.5			

Table 5. Sensitivity of each Colour-Filtered Wavelet Scalogram to Different Bearing Conditions

Bearing Condition	Colour Filter		
	Red	Green	Blue
Healthy	96.0	98.0	96.0
Rolling Element Fault	42.0	56.0	8.0
Inner Raceway Fault	82.0	58.0	96.0
Outer Raceway Fault	74.0	34.0	82.0

THE PROPOSED DECISION-MAKING MODEL

The previous section explained that each colour-filtered wavelet scalogram may be biased toward a certain bearing condition. However, fault classification based on an original wavelet scalogram (i.e. without a colour filter) does not guarantee a better classification accuracy. **Table 6** presents a confusion matrix of the original wavelet scalogram in the testing phase. The analysis results demonstrated that the classification accuracy is 67.5%, which is lower than the classification accuracy based on a red or blue colour-filtered wavelet scalogram. The authors believed that a better classification result could be obtained by treating each classification result from each colour-filtered wavelet scalogram as a piece of evidence that finally leads to an ultimate decision. **Figure 4** illustrates the proposed decision-making model flowchart. Basically, the training accuracy of each colour-filtered wavelet scalogram was calculated and assigned as a weighting function to each colour filter. This quantified the decision made by each colour filter. By combining each of these decisions, a better classification result can be obtained. **Table 7** presents a confusion matrix of the proposed decision-making model in the testing phase. The analysis results demonstrate that the RGB-filtered wavelet scalogram classification accuracy can be improved from an average of 68.5% to 77.5%. Therefore, the proposed decision-making model has been proven to be more superior, compared to a discrete decision made by each colour-filtered wavelet scalogram.

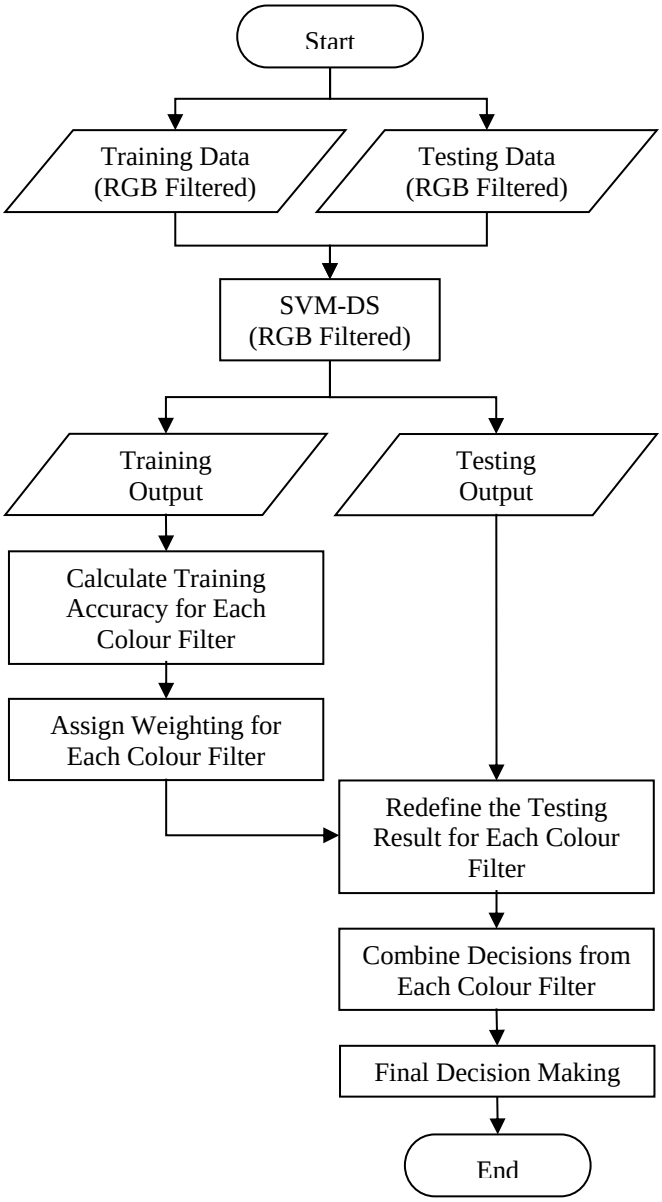

Figure 4 Flowchart of the Proposed Decision-Making Model

Table 6. Confusion Matrix for Testing Phase (Original Wavelet Scalogram)

Condition		Actual			
		1	2	3	4
Prediction	1 (healthy)	49	2	1	0
	2 (rolling element fault)	1	40	10	16
	3 (inner raceway fault)	0	3	38	26
	4 (outer raceway fault)	0	5	1	8
Sensitivity (%)		98.0	80.0	76.0	16.0
Accuracy (%)		67.5			

Table 7. Confusion Matrix for Testing Phase (the Proposed Decision-Making Model)

Condition		Actual			
		1	2	3	4
Prediction	1 (healthy)	50	1	0	0
	2 (rolling element fault)	0	26	5	11
	3 (inner raceway fault)	0	8	43	3
	4 (outer raceway fault)	0	15	2	36
Sensitivity (%)		100	52.0	86.0	72.0
Accuracy (%)		77.5			

CONCLUSION

This study presents the proposed decision-making model and demonstrates that combining each discrete decision made by each colour-filtered wavelet scalogram improves the accuracy of machinery fault classification. In addition, the human effort involved in interpreting a wavelet scalogram can be minimised or eliminated by a machine learning algorithm. This achievement also sheds new light on fault location identification and its severity by using a wavelet scalogram.

ACKNOWLEDGMENTS

The authors would like to extend their deepest gratitude to the Institute of Noise and Vibration UTM for funding the study under the Higher Institution Centre of Excellence (HICoE) Grant Scheme (R.K130000.7809.4J226, R.K130000.7843.4J227 and R.K130000.7843.4J228).

REFERENCES

Avci, E. (2013) 'A new method for expert target recognition system: Genetic wavelet extreme learning machine (GAWELM)', *Expert Systems with Applications*, 40(10), pp. 3984–3993. doi: 10.1016/j.eswa.2013.01.011.

Bayram, D. and Şeker, S. (2013) 'Wavelet-based Neuro-Detector for low frequencies of vibration signals in electric motors', *Applied Soft Computing*, 13(5), pp. 2683–2691. doi: 10.1016/j.asoc.2012.11.019.

Bhalla, D., Bansal, R. K. and Gupta, H. O. (2013) 'Integrating AI-based DGA fault diagnosis using Dempster–Shafer Theory', *International Journal of Electrical Power & Energy Systems*, 48, pp. 31–38. doi: 10.1016/j.ijepes.2012.11.018.

Browne, F. *et al.* (2013) 'Integrating textual analysis and evidential reasoning for decision making in Engineering design', *Knowledge-Based Systems*. Elsevier B.V., 52, pp. 165–175. doi: 10.1016/j.knosys.2013.07.014.

Cao, J. *et al.* (2013) 'Fault diagnosis of complex system based on nonlinear frequency spectrum fusion', *Measurement*. Elsevier Ltd, 46(1), pp. 125–131. doi: 10.1016/j.measurement.2012.05.028.

Du, W. *et al.* (2014) 'Wavelet leaders multifractal features-based fault diagnosis of rotating mechanism', *Mechanical Systems and Signal Processing*. Elsevier, 43(1–2), pp. 57–75. doi: 10.1016/j.ymssp.2013.09.003.

Guil, F. and Marín, R. (2013) 'A Theory of Evidence-based method for assessing frequent patterns', *Expert Systems with Applications*, 40(8), pp. 3121–3127. doi:

10.1016/j.eswa.2012.12.030.
He, Y.-L. *et al.* (2014) 'Bayesian classifiers based on probability density estimation and their applications to simultaneous fault diagnosis', *Information Sciences*. Elsevier Inc., 259, pp. 252–268. doi: 10.1016/j.ins.2013.09.003.
Hui, K. H. *et al.* (2017) 'Dempster-Shafer evidence theory for multi-bearing faults diagnosis', *Engineering Applications of Artificial Intelligence*. Elsevier, 57(November 2016), pp. 160–170. doi: 10.1016/j.engappai.2016.10.017.
Jamadar, I. M. and Vakharia, D. P. (2016) 'A Novel Approach Integrating Dimensional Analysis and Neural Networks for the Detection of Localized Faults in Roller Bearings', *Measurement*. Elsevier Ltd, 94, pp. 177–185. doi: 10.1016/j.measurement.2016.07.086.
Konar, P. and Chattopadhyay, P. (2011) 'Bearing fault detection of induction motor using wavelet and Support Vector Machines (SVMs)', *Applied Soft Computing*. Elsevier B.V., 11(6), pp. 4203–4211. doi: 10.1016/j.asoc.2011.03.014.
Li, P. *et al.* (2013) 'Multiscale slope feature extraction for rotating machinery fault diagnosis using wavelet analysis', *Measurement*. Elsevier Ltd, 46(1), pp. 497–505. doi: 10.1016/j.measurement.2012.08.007.
Natarajan, S. and Srinivasan, R. (2014) 'Implementation of multi agents based system for process supervision in large-scale chemical plants', *Computers & Chemical Engineering*. Elsevier Ltd, 60, pp. 182–196. doi: 10.1016/j.compchemeng.2013.08.012.
Ngui, W. K. *et al.* (2017) 'Blade fault diagnosis using artificial neural network', *International Journal of Applied Engineering Research*, 12(4), pp. 519–526.
Phillips, P. and Diston, D. (2011) 'A knowledge driven approach to aerospace condition monitoring', *Knowledge-Based Systems*. Elsevier B.V., 24(6), pp. 915–927. doi: 10.1016/j.knosys.2011.04.008.
Potes Ruiz, P. A., Kamsu-Foguem, B. and Noyes, D. (2013) 'Knowledge reuse integrating the collaboration from experts in industrial maintenance management', *Knowledge-Based Systems*. Elsevier B.V., 50, pp. 171–186. doi: 10.1016/j.knosys.2013.06.005.